Article ID: 1003－6326(2003)06－1301－05

Small angle X-ray scattering used in precipitation in AlZnMgCuLi alloy①

DU Zhi-wei(杜志伟)[1], ZHOU Tie-tao(周铁涛)[1], LIU Pei-ying(刘培英)[1], CHEN Chang-qi(陈昌麒)[1], ZHONG Hao(钟 皓)[2], HONG Xin-guo(洪新国)[2], ZHAO Hui(赵 辉)[2], DONG Bao-zhong(董宝中)[2]

(1. School of Materials Science and Engineering, Beijing University of Aeronautics and Astronautics, Beijing 100083, China;
2. Beijing Synchrotron Radiation Facility Division, Institute of High Energy Physics, Chinese Academy of Sciences, Beijing 100039, China)

Abstract: Small angle X-ray scattering has been used to study the variation of microstructure parameters in an Al-Zn-Mg-Cu-Li alloy aged at various temperatures for various durations. Coarsening of precipitates was studied by analyzing the curve of kinetics strength vs the cube of radius. The results show that the coarsening of precipitates conforms to LSW principle. In addition, the characteristic of $s^3J(s)$ vs s curves was analyzed. The results show that the curves for samples aged at 160 ℃ for various durations(24, 48 and 96 h) have negative deviation, which maybe results in the formation of certain new precipitate. In the other aging treatment states, the curves conform to Porod principle which means there is sharp boundary between the precipitates and matrix.

Key words: Al-Zn-Mg-Cu-Li alloys; precipitate; microstructure parameters; aging; small angle X-ray scattering

CLC number: TG 113.12; TG 115.221 **Document code:** A

1 INTRODUCTION

7XXX series alloys are used extensively in aerospace industry. In recent years, developing high strength and low density materials is the main aim for most researchers. Al-Li alloys have many merits such as high specific strength, high specific modulus and low density. In order to take advantage of Al-Li alloys' merits, Li has been added to normal aluminum alloy. Many new alloy systems were developed such as Al-Cu-Li, Al-Cu-Mg-Li and Al-Mg-Li alloys[1]. Many studies have also been focused on 7XXX series (Al-Zn-Mg-Cu) containing Li. The precipitation sequence in AlZnMgCuLi alloys under various aging conditions is of prime importance for the understanding of their mechanical strength and corrosion resistance properties. Much of the research to date has been dedicated to the time evolution of the microstructure of this alloy by transmission electron microscopy[1-4]. In this study we used the small angle X-ray scattering measurement to obtain the quantitative information about precipitate size range and volume fraction under various aging conditions. This information obtained will be beneficial to deep understanding the precipitation process of AlZnMgCuLi alloys.

2 EXPERIMENTAL

The composition of the alloys(mass fraction, %) is Zn 5.14, Mg 1.24, Cu 1.76, Li 1.01, Mn 0.35, Zr 0.10, Cr 0.24. The alloy was solution treated at 490 ℃ for 1 h in salt bath followed by water quenching. Several aging heat treatments were then performed under different conditions.

Small angle X-ray scattering measurements were performed at BSRF Division, Institute of High Energy Physics. The gauge of samples was 8 mm × 6 mm × 0.07 mm. The parameters of light source near samples were as follows: energy range is 3－12 keV, energy resolution $\Delta E/E$ about 2×10^{-4}, photons flux 1.0×10^{10} s^{-1}, wavelength of X-ray 0.154 nm and facula size 3.2 mm × 1.5 mm. Scattering signal was recorded by detector of formation image board.

3 RESULTS

3.1 Determination of precipitate radius

According to the small angle X-ray scattering intensity obtained by experiments, we can obtain the relation curves of the relative scattering intensity(J_h) and scattering vector (h) which are shown in Fig. 1.

For SAXS, it is assumed that the system formed by precipitates and matrix is sparse and homogeneous system . According to Guinier approximate formula , scattering intensity is as fol-

① **Foundation item:** Project(G19990649) supported by National Key Fundamental Research and Development Program of China and project (2001AA332030) supported by Advanced Materials Committee of China

Received date: 2002－12－24; **Accepted date:** 2003－02－22

Correspondence: DU Zhi-wei, Candidate for PhD; Tel: +86-13520436981, +86-10-82314488; E-mail: zhiweidu110@sohu.com, zhiweidu110@sina.com

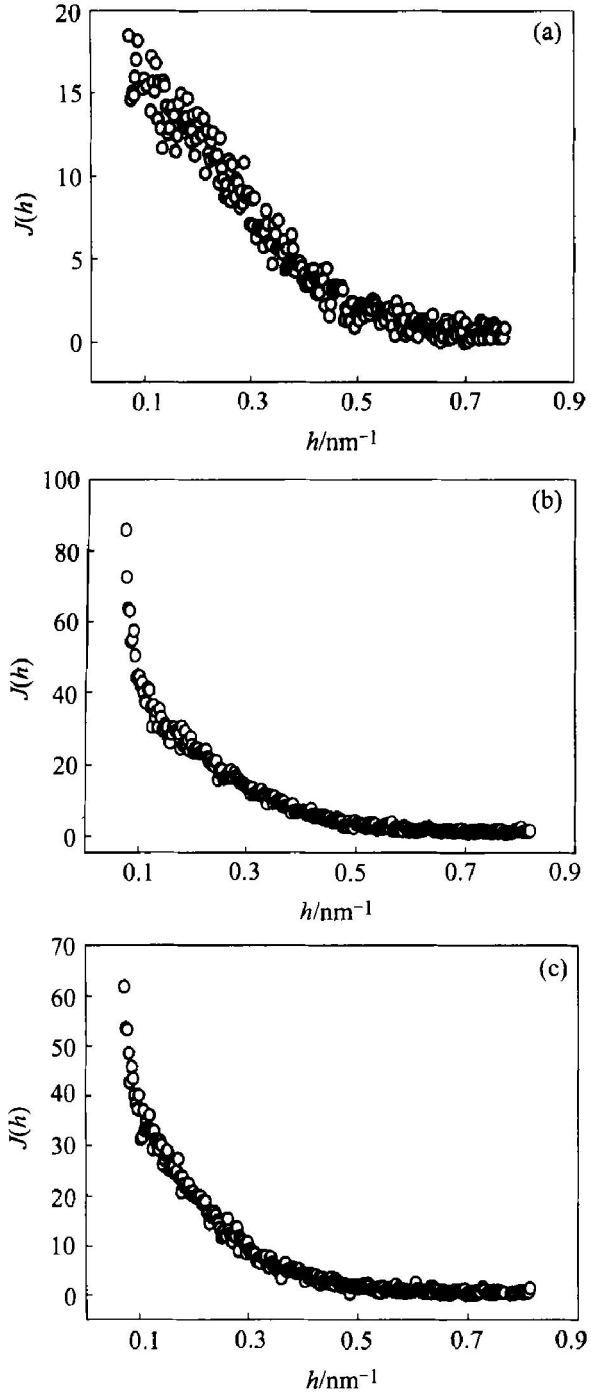

Fig. 1 Curves of $J(h)$ vs h for alloys aged under various conditions
(a) —Aged at 160 ℃ for 24 h;
(b) —Aged at 160 ℃ for 48 h;
(c) —Aged at 160 ℃ for 96 h

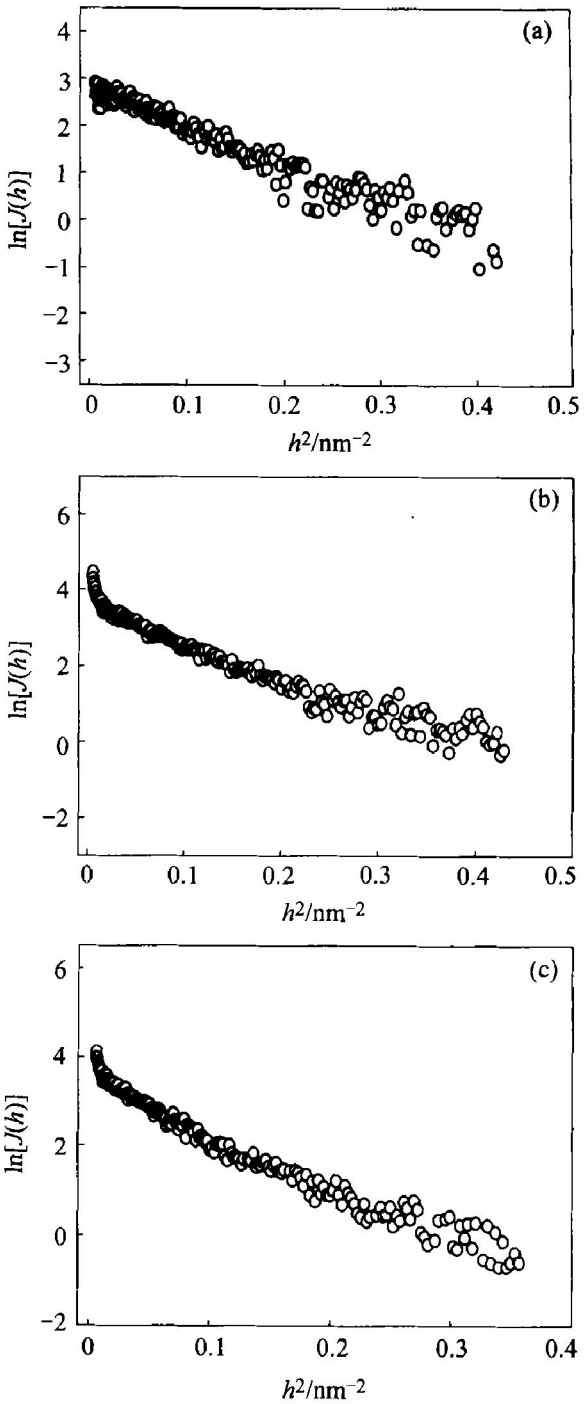

Fig. 2 Curves of $\ln J(h)$ vs h^2 for alloys aged under various conditions
(a) —Aged at 160 ℃ for 24 h;
(b) —Aged at 160 ℃ for 48 h;
(c) —Aged at 160 ℃ for 96 h

lows[5-7]:

$$J_h = J_e N n^2 e^{-R_G^2 h^2/3} \quad (1)$$

where J_h is the scattering intensity corrected collimation error, J_e the scattering intensity of an electron, n the total electron number of one particle, N the total particle number in the field irradiated by X-ray, R_G the gyration radius of particles, h the scattering vector. To obtain $\ln J(h) - h^2$ curves, we can use the experimental data $J(h)$ to substitute J_h. J_h is the relative intensity, which is calculated by subtracting background intensity from the scattering intensity of samples. The curves of $\ln J(h)$ vs h^2 are shown in Fig. 2. α is the slope of $\ln J(h) - h^2$ curves in the range of small angle. With formula $R_G = (-3\alpha)^{1/2}$, the gyration radius of precipitates can be calculated at different heat treatment states. The values are listed in Table 1. Most of the precipitates are spherical based on the observation of TEM[8,9]. Then the practical radius can be calculated from the equation which describes the relation between the practical radius and the gyration radius

$$R_G = \sqrt{3/5}R \quad (2)$$

3.2 Determination of Porod constant

As shown in Fig. 3, $s^3J(s)-s$ curves are plotted. It can be seen from Fig. 3 that $s^3J(s)$ approaches a constant K'_p at large values of s for samples aged at 130 ℃ for 24 h, 150 ℃ for 24 h and two-step aging at 120 ℃ for 3.5 h then at 160 ℃ for 15 h, respectively. This indicates that there is sharp boundary between precipitates and matrix in electron density. Porod constant can be expressed as follows[5]:

$$\lim_{s\to\infty}[s^3J(s)] = K'_p \quad (3)$$

where $s = 2\sin\theta/\lambda$, 2θ is scattering angle, λ wavelength of X-ray and $J(s)$ the scattering intensity obtained by using a long slit collimation system and K'_R Porod constant. However, it can be seen from Fig. 3 that $s^3J(s)-s$ curve has negative deviation at large values of s for samples aged at 160 ℃ for 96 h. In Ref. [5], the deviation stems from obscure boundary between precipitates and matrix. It means that there is an transitional zone of electron density between two phases.

When $s^3J(s)-s$ curves are in conformity with Porod principle, K'_p is related to specific inner S_p surface of particle-matrix two-phase system. The relation is given by Eqn. (4)[5,6,10]

$$S_p = 8\pi K'_p/[(J_e(\Delta\rho)^2 V] \quad (4)$$

where J_e is the scattering intensity of an electron, $\Delta\rho$ electron density difference between the particle and the matrix and V the volume of samples irradiated by X-ray. In certain condition $[J_e(\Delta\rho)^2 V]$ is an constant. Specific inner surface S_p of particle-matrix two-phase system, i e, the ratio of the total surface area of particles to the volume of samples, is directly related to material property. However, it is difficult to calculate directly. It can be seen from Eqn. (4) that K'_p values reflect the relative values of specific inner surface. The values of K'_p are listed in Table 1.

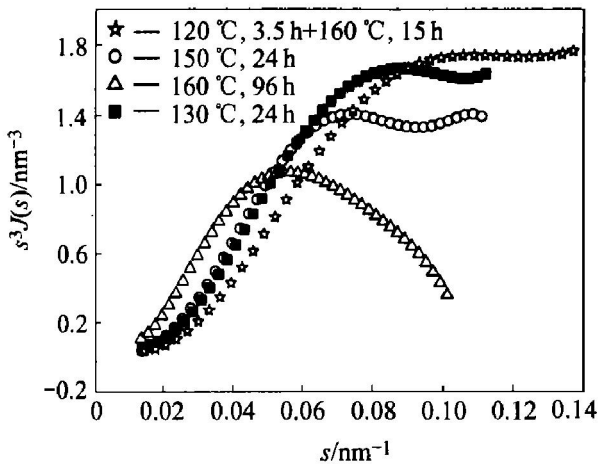

Fig. 3 Curves of $s^3J(s)$ vs s for alloys aged under various conditions

3.3 Determination of integrated intensity

With long slit collimation system, the integrated intensity can be written as follows[5,6]:

$$\tilde{Q}_s = \int_0^\infty sJ(s)\,ds = I_e(\Delta\rho)^2 V\varphi(1-\varphi) \quad (5)$$

where $\Delta\rho$ is electron density difference between the particle and the matrix, V the volume of samples irradiated by X-ray and φ the volume fraction of particles that is the volume ratio of particles to the sample.

Integrated intensity has important physical meaning. It is only dependent on the volume fraction φ when parameters V and $\Delta\rho$ are fixed. In order to obtain the relative values of volume fraction, we can calculate the values of $\tilde{Q}_s$ firstly. By comparing $\tilde{Q}_s$, we can understand the variation of volume fraction. To calculate $\tilde{Q}_s$ accurately, Eqn. (5) can be rewritten as follows:

$$\tilde{Q}_s = \int_0^{s_1} sJ(s)\,ds + \int_{s_1}^{s_2} sJ(s)\,ds + \int_{s_2}^\infty sJ(s)\,ds = \tilde{Q}_1 + \tilde{Q}_2 + \tilde{Q}_3 \quad (6)$$

where $\tilde{Q}_1 = \int_0^{s_1} sJ(s)\,ds$, $\tilde{Q}_2 = \int_{s_1}^{s_2} sJ(s)\,ds$, $\tilde{Q}_3 = \int_{s_2}^\infty sJ(s)\,ds$. In the range $s_1 - s_2$, the scattering in-

Table 1 Values of α, R_G, R, K'_p, $\tilde{Q}_s$ of samples heat treated under various conditions

No.	Heat treatment	α	R_G/mm	R/nm	K'_p/nm^{-3}	$\tilde{Q}_s$/nm^{-2}
1	490 ℃, 1 h+ 160 ℃, 24 h	− 9.612	5.37	6.93		
2	490 ℃, 1 h+ 160 ℃, 48 h	− 13.146	6.28	8.11		
3	490 ℃, 1h+ 160 ℃, 96 h	− 16.756	7.09	9.15		
4	490 ℃, 1h+ 120 ℃, 96 h	− 3.266	3.13	4.04	0.001 4	0.029 8
5	490 ℃, 1h+ 120 ℃, 24 h+ 180 ℃, 3 h	− 13.063	6.26	8.08	0.000 7	0.031 4
6	490 ℃, 1 h+ 130 ℃, 24 h	− 6.279	4.34	5.60	0.014 2	0.044 5
7	490 ℃, 1 h+ 150 ℃, 24 h	− 7.712	4.81	6.20	0.001 2	0.039 2
8	520 ℃, 40 min+ 120 ℃, 3.5 h+ 160 ℃, 15 h	− 4.588	3.71	4.78	0.001 6	0.038 9

tensity can be obtained directly from experiments. In the range $0 - s_1$, the scattering intensity can be obtained by extrapolation of $J(s)$ values from $s_1 - s_2$. In the range $s_2 - \infty$, $\int_{s_2}^{\infty} sJ(s)\mathrm{d}s$ can be rewritten as follows according to Eqn. (3):

$$\tilde{Q}_3 = \int_{s_2}^{\infty} sJ(s)\mathrm{d}s = \int_{s_2}^{\infty} K'_{\mathrm{p}} s^2 \mathrm{d}s = K'_{\mathrm{p}} s_2 \quad (7)$$

The values of $\tilde{Q}_s$ calculated by Eqn. (6) are listed in Table 1.

4 DISCUSSION

On the basis of the former work[8, 9], it is considered that the strengthening phase is mainly metastable η′ phase for the experimental alloy. In this alloy, the content of zinc is relatively high and that of lithium is 1.01%. It is often considered that lithium mostly exists in solid solution and GP zones. There is no existence of large Al_3Li. Furthermore, due to high binding energy of lithium-vacancy, the lithium-vacancy couples will form earlier. The diffusion velocity of Mg and Zn atoms is reduced.

After the isothermal aging heat treatments under various conditions, the coarsening process of precipitates can be described by LSW(Lifshitz-Slyozov-Wangner) model[4, 11]. The LSW model for coarsening kinetics is given by Eqn. (8) which predicts the time dependence of the radius of spherical precipitates

$$R^3 - R_0^3 = Kt$$
$$K = 8\Omega^2 \gamma c_e D/(9k_B T) \quad (8)$$

where R_0 and k_B are constants, γ the precipitate-matrix interface energy, Ω the average atomic volume, c_e the equilibrium solute concentration, and D the solute diffusion coefficient. It becomes then possible to gather all experimental results, for various times t and temperature T, on a master plot by the use of a scaling variable:

$$K_s = \int \frac{\mathrm{d}t}{T(t)} \mathrm{e}^{-Q/k_B T(t)} \quad (9)$$

we call this variable "kinetic strength" as first suggested by Shercliff and Ashby[4, 11]. The kinetic strength characterizes the advance of coarsening that results from a given aging treatment.

As shown in Fig. 4, the increase of R^3 with variable K_s follows a linear relationship. So the coarsening of precipitates conforms to the principle of LSW.

From the radius listed in Table 1, we can see the variation of radius is dependent on the temperature. The radius increases with increasing the temperature when samples are aged for the same durations.

The values of the Porod constant K'_{p} and integrated intensity $\tilde{Q}_s$ of samples aged at 130 ℃ and 150 ℃ for 24 h is respectively 1.42×10^{-2}, 1.2×10^{-3} and 4.45×10^{-2}, 3.92×10^{-2}. This indicates that the values decrease with increasing temperature. By analyzing, it is considered that the quantity of precipitation is near equilibrium aged at higher temperature for 24 h. The system with disperse precipitates has high interface energy, so the system is instable. The precipitates will coarsen by large particles growing and small particles dissolving, which is called Ostwald ripening mechanism. The process of coarsening is related to Gibbs-Thomson effect[12]. According to this effect, the solute concentration in matrix near particles is dependent on the curvature radius of particles. The solubility of large particles is lower than that of the small particles. So there is a concentration gradient in the matrix between two kinds of particles, which make solute flow from small particle to the large. This competitive growth process maybe leads to the decrease of specific inner surface and volume fraction.

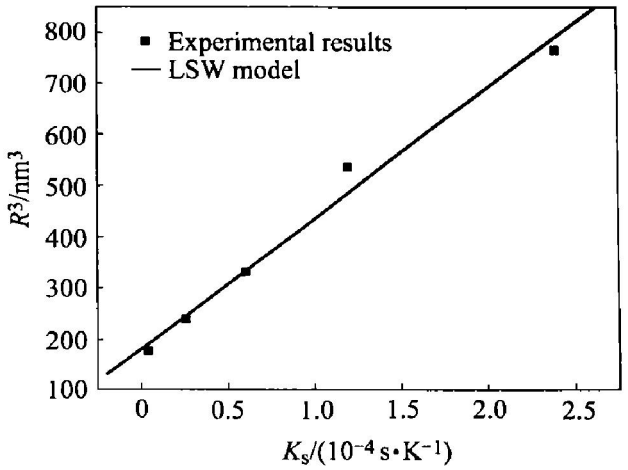

Fig. 4 Curve of R^3 vs K_s for alloys aged under various conditions

It is shown in Fig. 3 that $s^3J(s)$ approaches a constant at large values of s for the samples aged at 130 ℃ for 24 h, 150 ℃ for 24 h and two-step aging at 120 ℃ for 3.5 h then 160 ℃ for 15 h, respectively. The curves for the samples aged at 120 ℃ for 96 h then two-step aging at 120 ℃for 24 h and at 180 ℃ for 3 h respectively, have the same character, which are not listed one by one. This indicates there is sharp boundary between the precipitates and matrix[5, 6, 10]. It is also shown in Fig. 3 that the $s^3J(s)$ —s curve has negative deviation for sample aged at 160 ℃ for 96 h. The curves for samples aged at 160 ℃ for 24 h and 48 h respectively, are similar to those aged at 160 ℃ for 96 h which are not listed here. This maybe results in the formation of certain new precipitate, which forms the new transitional interface layer between the matrix and precipitates. This problem needs to be verified by transmission electron mi-

croscopy(TEM).

5 CONCLUSIONS

1) From the precipitate radius deduced from the SAXS measurement, it appears that the coarsening of precipitates conforms to LSW principle.

2) The variation of precipitate radius is dependent on the temperature, which increases with increasing the temperature aged for the same durations.

3) The $s^3J(s)-s$ curves aged at 160 ℃ for various durations(24, 48 and 96 h) have negative deviation, which maybe results in the formation of certain new precipitate. In the other aging treatment states, $s^3J(s)-s$ curves conform to Porod principle which means there is sharp boundary between the precipitates and matrix.

REFERENCES

[1] Gu Y J, Wahab A, Huang Z, et al. The structure transformation in an Al-Li-Zr-Mg-Cu-Zr alloy[J]. Mater Sci Eng A, 2001, A316: 39-45.

[2] Gomiero P, Reeves A, Pierre A. In situ small angle X-ray scattering(SAXS) study of precipitation in Al-Zr-Mg-Cu alloy[A]. The 4th International Conference on Aluminum Alloys[C]. 1994. 644-651.

[3] Werenskiold J C, Deschamps A, Brechet Y. Characterization and modeling of precipitation kinetics in an Al-Zr-Mg alloys[J]. Mater Sci Eng A, 2000, A293: 267-274.

[4] Guyot P, Cottignies L. Precipitation kinetics, mechanical strength and electrical conductivity of AlZnMgCu alloys[J]. Acta Mater, 1996, 44(10): 4161-4167.

[5] MENG Zhao-fu. Theory and Application of Small Angle X-ray Scattering[M]. Changchun: Jilin Science and Techonology Press, 1995. (in Chinese)

[6] MENG Zhao-fu, DENG Yong, LONG Hou-wen. Study of the hardness change of Al-Zn-Mg alloy during retrogression reaging treatments[J]. Acta Metall Sinica, 1997, 33(5): 479-483. (in Chinese)

[7] MENG Zhao-fu. Determination of three activation energy of non-crystal alloy by small angle X-ray scattering[J]. Science in China(Series A), 1994, 24(7): 761-767. (in Chinese)

[8] BAI Pu-cun, WEI Fang, ZHOU Tie-tao, et al. Influence of Li on structures properties of Zn-rich Al-Zn-Mg-Cu alloy[J]. The Chinese Journal of Nonferrous Metals, 2002, 12(Al Special): 172-175. (in Chinese)

[9] BAI Pu-cun, ZHAO Zhong-kui, ZHOU Tie-tao, et al. Influence of Li on precipitation process of 7XXX aluminum alloy[J]. The Chinese Journal of Nonferrous Metals, 2002, 12(Al Special): 176-179. (in Chinese)

[10] MENG Zhao-fu, WANG Yu-ming. Study of interface between crystal phase and non-crystal phase of non-crystal alloy during tempering[J]. Science in China(Series A), 1990(11): 1224-1228. (in Chinese)

[11] Cottignies L, Guyot P. Precipitation kinetics and strengthening in AlZnMgCu alloys[J]. Mater Sci Forum, 1996, 217-222: 1263-1268.

[12] YU Yong-ning. Metallurgical Principle[M]. Beijing: Metallurgical Industry Press, 2000. 498. (in Chinese)

(Edited by HUANG Jin-song)